

Carrie Langston<sup>1</sup>, Jian Zhang<sup>1</sup>, Ken Howard<sup>2</sup>

<sup>1</sup>Cooperative Institute for Mesoscale Meteorological Studies, Norman, OK

<sup>2</sup>NOAA/National Severe Storms Laboratory, Norman, OK

## 1. INTRODUCTION

The aviation community and electrical power commercial sector have a need for rapidly updating WSR-88D radar data spanning across regions in a seamless mosaicked network. Early radar mosaic products, mainly in 2-D and with just 16 data levels, have provided users a useful tool to monitor weather systems in a regional and national domain. Recently, 3-D multiple radar mosaics (Zhang et al. 2004) were developed for quantitative precipitation estimation and for convective numerical weather prediction models' data assimilation and for other applications. The National Severe Storms Laboratory (NSSL) has development an algorithm, Four-Dimensional Dynamic Grid (4DDG), designed to accurately and rapidly represent radar data over a given 4-D domain and incorporates the operational nuisances of WSR-88D.

The 4-D dynamic mosaic is a 3-D Cartesian grid that updates whenever a new tilt of data becomes available from any radar that covers the analysis domain. For a domain with 10 radars running VCP11, the update rate can be as high as every 3 seconds. The higher update frequency can assist towards improving lead and response times for severe weather identification.

The 4DDG algorithm is presented in section 2, its weighting schemes in section 3 through 5, and preliminary results in section 6.

## 2. ALGORITHM

4DDG is a continuous algorithm that ingests base level volumetric reflectivity data from multiple radars as it becomes available, remaps and mosaics it to a common Cartesian grid, and continuously updates a 3-D grid of the reflectivity stored in shared memory.

Upon ingesting a tilt of polar data, 4DDG determines what grid cells are affected by the new data and uses a Barnes weighting scheme to apply new radar data to the 3-D grid,

$$Z_m = \frac{\sum_{i=1}^N \left( \sum_{t=1}^T w_{g,t}^i Z_{g,t}^i \right)}{\sum_{i=1}^N \left( \sum_{t=1}^T w_{g,t}^i \right)} \quad (1)$$

where  $Z_m$  is the mosaic reflectivity at a given grid cell,  $N$  is the number of observed reflectivity values affecting a given cell within the 3-D space  $\Omega[x,y,z]$ ,  $T$  is the number of observed reflectivity values at a given cell over some history,  $Z_{g,t}^i$  is the observed reflectivity from a radar in  $\Omega[x,y,z]$  at time  $t$ , and  $w_{g,t}^i$  is the weight of each reflectivity value with respect to a given grid cell at time  $t$ .

The weight  $w_{g,t}^i$  is a combination of remap, mosaic, and temporal weights. Dropping the subscript  $t$  and superscript  $i$ , the weight from equation (1) is expanded to

$$W_g = W_{remap} \bullet W_{mosaic} \bullet W_t \quad (2)$$

where  $W_{remap}$  is the spatial weighting function for remapping a single radar reflectivity field from spherical to Cartesian coordinates,  $W_{mosaic}$  is the spatial weighting function for mosaicking multiple radar reflectivity values, and  $W_t$  is the temporal weighting function.

Detailed descriptions of the weights of equation (2) are found in the following sections.

## 3. REMAP WEIGHTING SCHEMES

Several difficulties are associated with remapping polar radar data to Cartesian coordinates given the nature of radar data and the spherical coordinates of radar observations. Different remapping schemes perform better in different scenarios. 4DDG is capable of applying three different remapping schemes depending on a user-defined option. All three methods calculate the components of  $W_{remap}$  that contribute to equation (1) and (2), either explicitly or implicitly. The calculation of  $W_{remap}$  is based on

$$W_{remap} = W_r \bullet W_\phi \bullet W_\theta \quad (3)$$

where  $w_r$  is a radar bin's weight with respect to range,  $w_\phi$  is the weight with respect to azimuth, and  $w_\theta$  is the weight with respect to elevation angle.

Each method is optimal given certain conditions. The various methods and the conditions for which they are optimal are outlined in sub-sections 3.1 through 3.3.

Corresponding author address: Carrie Langston, NSSL, 1313 Halley Circle, Norman, OK 73069.

Email: [carrie.langston@noaa.gov](mailto:carrie.langston@noaa.gov)

Sub-section 3.4 discusses the problem of remapping and over-sampling.

### 3.1 NEAREST NEIGHBOR

Nearest neighbor (NN) is the simplest remapping scheme and the most suited for research purposes. Each grid cell in the 3-D domain is assigned a reflectivity value based on the radar bin closest to it. Determining which radar bin is closest is a combination of radar beam propagation and great circle geometry. The reflectivity value of one radar bin has full sway over the grid cell's reflectivity value for remap purposes. The weights listed in equation (3) are implicitly set, giving them a value of one.

The NN method works to reduce the number of gaps between radar observations, but it does not eliminate them. Discontinuities and ring-shaped artifacts are still present in the remapped field (Zhang 2004). Such discontinuities and artifacts make NN unsuitable for radar analysis but helpful for research and development.

### 3.2 1-D VERTICAL LINEAR INTERPOLATION

The second remapping scheme is a combination of 1-D vertical linear interpolation (VI) and NN approaches. VI actually interpolates with respect to the elevation angle direction. The term "vertical" is used since, at low values, the elevation angle direction is adequately approximated by the vertical direction (Zhang 2004).

Initially, this method uses radar beam propagation and great circle geometry to determine a grid cell's position with respect to the given radar,  $(\phi, r, \theta)$ . The grid cell's azimuth and range are set to the closest corresponding radar bin. Thus, the azimuthal and range components of equation (3) are set to a value of one via NN.

The elevation angle of the grid cell with respect to the radar ( $\theta$ ) is framed by the tilt directly above ( $\theta_2$ ) and below ( $\theta_1$ ) it as indicated by the radar's VCP mode. These three elevation angles are used to compute the linear interpolation weights for  $w_\theta$ . Fig. 1 illustrates the vertical interpolation aspect of this option.

The weights for  $w_\theta$  are computed using,

$$w_{\theta_1} = \frac{\theta - \theta_1}{\theta_2 - \theta_1} \quad (4a)$$

$$w_{\theta_2} = \frac{\theta_2 - \theta}{\theta_2 - \theta_1}, \quad (4b)$$

where  $w_{\theta_1}$  and  $w_{\theta_2}$  are the linear interpolation weights for reflectivity values at  $(\phi, r, \theta_1)$  and  $(\phi, r, \theta_2)$ , respectively.

The combination of vertical linear interpolation and nearest neighbor techniques is capable of removing more discontinuities than NN alone. It is well suited for weather events involving convective storms, whose

vertical structure can be more consistently represented by vertical interpolation. The presence of ring-shaped artifacts is reduced using this method but are still present for weather events involving stratiform precipitation whose structure is more horizontal (Zhang 2004).

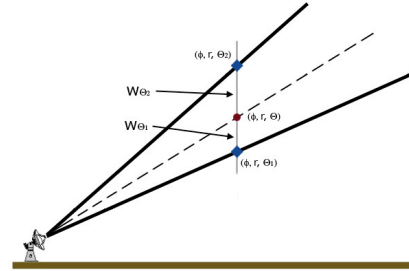


Fig. 1 4DDG's 1-D vertical linear interpolation between tilts computes weights with respect to the elevation angle to determine the reflectivity at point  $(\phi, r, \theta)$ .

### 3.3 2-D HORIZONTAL LINEAR INTERPOLATION

The final remap option for 4DDG is a combination of 2-D horizontal linear interpolation (HI) and VI as described in section 3.2. The 2-D horizontal interpolation will effect the weights  $w_\phi$ ,  $w_r$ , and  $w_\theta$  of equation (3) while VI will effect  $w_\theta$  of equation (3).

Radar beam propagation and great circle geometry are used to calculate the grid cell's location,  $(\phi, r, \theta)$ . The grid cell's position is framed by surrounding elevation angles, ranges, and azimuths to create a 3-D box around the grid cell. Fig. 2 illustrates HI and the azimuth/range/elevation angle 3-D frame surrounding the grid point.

HI is performed on a horizontal plane defined in spherical coordinates, which is a function of range and elevation angle. In this respect, HI is partially responsible for the value of  $w_\theta$  in equation (3). The grid cell's elevation angle  $\theta$  is framed by the tilt directly above ( $\theta_2$ ) and below ( $\theta_1$ ) it. Using elevation angles  $\theta_1$  and  $\theta_2$ , the range of a radar bin at the same height as the grid point is derived via radar beam propagation and great circle geometry. Weight calculations for HI with respect to range are,

$$w_{r_1} = \frac{r_1 - r}{r_1 - r_2} \quad (5a)$$

$$w_{r_2} = \frac{r - r_2}{r_1 - r_2} \quad (5b)$$

where,  $w_{r_1}$  and  $w_{r_2}$  are linear interpolation weights for the reflectivity values at  $(\phi, r_1, \theta_2)$  and  $(\phi, r_2, \theta_1)$ , respectively.

HI defines the azimuthal portion ( $w_\phi$ ) of the 2-D interpolation by framing the grid point's azimuth ( $\phi$ ) by the radial behind it ( $\phi_1$ ) and before it ( $\phi_2$ ). Weight calculations for HI with respect to azimuth are

$$w_{\phi_1} = \frac{\phi_1 - \phi}{\phi_2 - \phi_1} \quad (5c)$$

$$w_{\phi_2} = \frac{\phi_2 - \phi}{\phi_2 - \phi_1} \quad (5d)$$

where,  $w_{\phi_1}$  and  $w_{\phi_2}$  are linear interpolation weights for the reflectivity values at  $(\phi_1, r, \theta)$  and  $(\phi_2, r, \theta)$ , respectively.

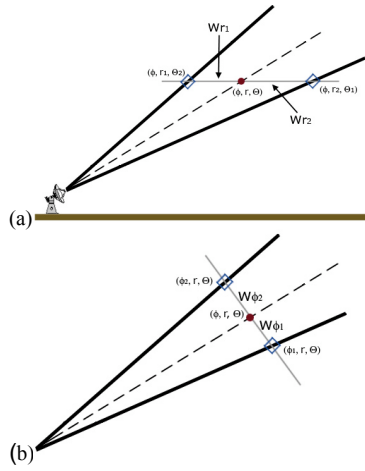


Fig. 2 Illustration of 2-D horizontal linear interpolation weights and parameters with respect to range and elevation angle (a) and with respect to azimuth (b). For both (a) and (b), diamond shaped boxes indicate reflectivity values on the polar grid. Dots represent the grid point  $(\phi, r, \theta)$  whose value is interpolated. All points are referenced in polar coordinates.

When combined with reflectivity values, the weights from equation (5), form the two-dimensional linear interpolation equation

$$\begin{aligned} z_i = & w_{r_2} \cdot w_{\phi_2} \cdot z_k + w_{r_2} \cdot w_{\phi_1} \cdot z_{k+1} \\ & + w_{r_1} \cdot w_{\phi_2} \cdot z_{k+nx} \\ & + w_{r_1} \cdot w_{\phi_1} \cdot z_{k+nx+1} \end{aligned} \quad (6)$$

where  $z_i$  is the interpolated reflectivity value for the grid point and  $z_k$ ,  $z_{k+1}$ ,  $z_{k+nx}$ , and  $z_{k+nx+1}$  are the radar reflectivity values at points  $(\phi_2, r_2, \theta_1)$ ,  $(\phi_1, r_2, \theta_1)$ ,  $(\phi_2, r_1, \theta_2)$ , and  $(\phi_1, r_1, \theta_2)$ , respectively.

The combination of horizontal and vertical linear interpolation removes discontinuities in the radar reflectivity field and greatly reduces the number of ring-shaped artifacts for stratiform weather events. However, the horizontal interpolation component can have an adverse effect when applied to convective

storm environments. The vertical structure of convective storms is smeared horizontally (Zhang 2004). Therefore, this final method is desirable for stratiform weather events only.

### 3.4 OVER-SAMPLING WEIGHTING SCHEMES

Sub-sections 3.1 through 3.3 discussed remapping weight formulas and methods used in 4DDG, where it is assumed that the size of a grid cell is less than the size of a radar bin (under-sampled). However, grid cells that are located close to a radar may be over-sampled. This phenomenon results from the nature of radar data in spherical coordinates. The azimuthal resolution of radar data is better than one kilometer within 60 kilometers of the radar. Within this bound it is possible for a grid cell, which is one kilometer squared, to be sampled by more than one radar bin of reflectivity. The previously discussed remap weighting schemes do not take into account this possibility. Therefore, some reflectivity values maybe missed. Fig. 3 illustrates a simple example of radar over-sampling.

To avoid losing the additional data available from over-sampling, 4DDG may employ one of two methods for use in calculating a final reflectivity value for over-sampled grid cells. These two methods are arithmetic mean and linear interpolation. Note the over-sampling weight is incorporated as part of the remapping weight.

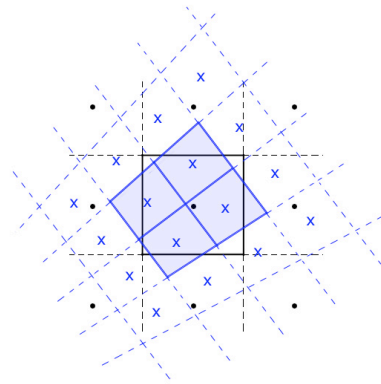


Fig. 3 Overlay of polar and Cartesian grids illustrating the over-sampling problem. The Cartesian grid cell centers are marked by dots and the polar bin centers by x's. The shaded polar bins are those that sample the grid cell of interest, which is outlined in solid black.

The arithmetic mean method assigns a weight of one to  $w_\phi$ ,  $w_r$ , and  $w_\theta$  for each radar bin whose center falls within the grid cell. These weights, when applied in equation (3) and then equation (1), result in 4DDG calculating a grid cell's reflectivity using a mean reflectivity as seen in

$$z_i = \frac{1}{n} \sum_{k=0}^n z_k \quad (9)$$

where  $z_i$  is the mean reflectivity value at a given grid cell,  $z_k$  is the reflectivity of  $k^{\text{th}}$  radar bin associated with the grid cell, and  $n$  is the number of reflectivity bins associated with the grid cell.

Over-sampling in 4DDG can also be handled by a linear interpolation method. Radar bins whose centers are located in an over-sampled grid cell are weighted based on their position with respect to the grid cell's center. The influence a radar bin has on the grid cell is determined by

$$w = 1 - \frac{d}{R} \quad (10)$$

where  $w$  is the resultant weight,  $d$  is the distance between each radar bin center and grid cell center, and  $R$  the radius of influence equal to the cross-diagonal distance of one kilometer cubed (approximately the size of one grid cell).

#### 4. MOSAIC WEIGHTING SCHEMES

In addition to remapping radar data, 4DDG must also mosaic it. Mosaicking radar data is necessary when more than one radar polar field contains observations for the same grid point. A methodology is required to determine how multiple values will be utilized.

4DDG uses a simple weighting scheme based on the observation's distance from the radar. An observation closer to its respective radar is believed more accurate and receives a higher weight. Equation (7) is the exponential decaying weighting function used by 4DDG for mosaicking.

$$w_{\text{mosaic}} = \exp\left(-\frac{r^2}{R^2}\right) \quad (7)$$

Here,  $r$  is the distance of the observation from its respective radar and  $R$  is an adaptable length scale (i.e., 25 km).

The nature of exponentially decaying functions is especially useful for radar analysis such as 4DDG where it is important to retain information pertaining to storm severity (i.e., maximum reflectivity magnitude). The shape of an exponential weighting function is easily adjustable to achieve a rapid decrease with range while remaining a positive weight value. The rapid decreasing weight is important for retaining high-resolution features in raw radar data at close ranges. A positive weight value for long ranges is important to assure the radar has influence over the entire region it covers. Other weighting functions such as linear or Cressman do not have both of these key features at the same time.

#### 5. TEMPORAL WEIGHTING SCHEMES

This section addresses 4DDG's temporal weighting scheme. Limited research exists in studying the effects of different temporal weighting schemes on mosaicked reflectivity. Therefore, in an initial effort, 4DDG uses the exponentially decaying weighting function

$$w_t = \exp\left(-\frac{t^2}{T^2}\right) \quad (8)$$

where  $t$  is the age of the reflectivity data and  $T$  is an adaptable time decaying scale. A decaying weighting function was used so that new data receives larger weights than old data associated with the same grid cell. The decaying scale should be related to the life cycles of storms. Preliminary tests using a value of 2 minutes on convective storms show that the temporal weighting function provides consistent analysis in time (see section 6). Further investigation is required to find the optimal values of the decaying scale for different storm systems.

#### 6. PRELIMINARY RESULTS

In this section preliminary results are shown for 4DDG. Highlighted here is an Oklahoma case on 14 August 2002. Data from WSR-88D radars KTLX and KFDR were input into 4DDG in a tilt-by-tilt time sequential order. Fig. 4 defines a vertical cross-section and the domain used for this case. Output from 4DDG is displayed using Vis5D software (<http://www.ssec.wisc.edu/~billh/vis5d.html>).

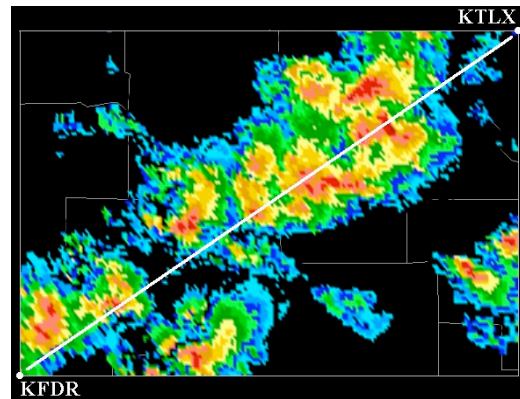


Fig. 4 Definition of the vertical cross-section seen in Fig. 5 and Fig. 6. Reflectivity data shown is a horizontal cross-section at an elevation of 3.6 km from a mosaicked 3-D reflectivity on 14 August 2002 at 0223 UTC.

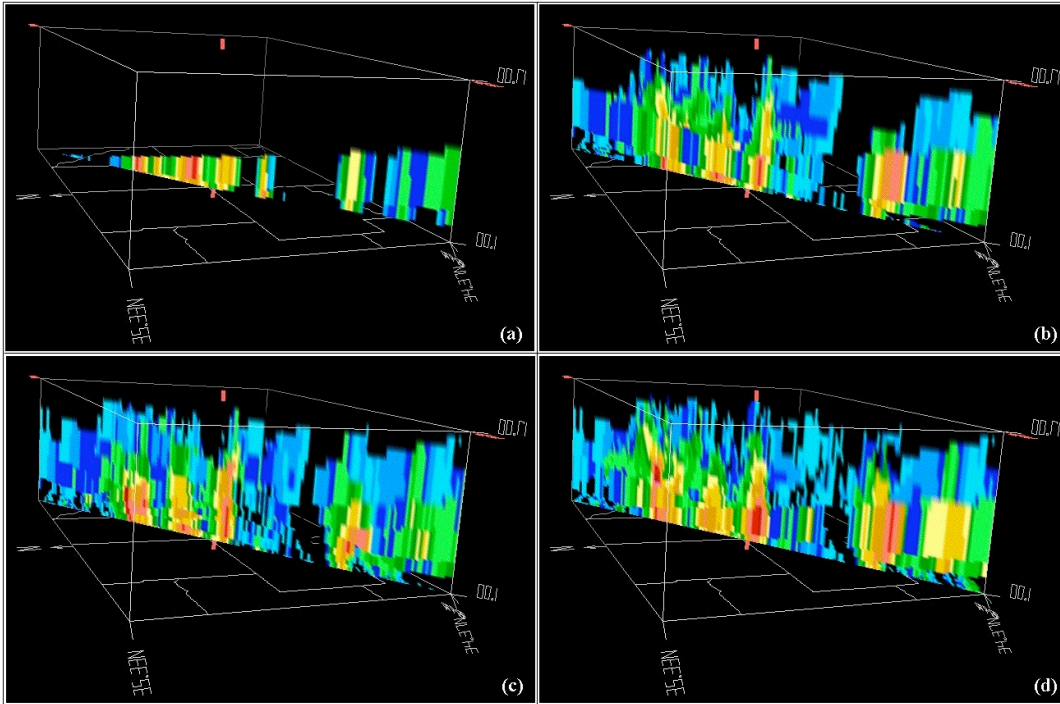


Fig. 5 4DDG output, with temporal weighting turned off, using KTLX and KFDR data on 14 August 2002. Shown is a vertical cross-section of 3-D reflectivity with endpoints at KTLX and KFDR at 0217 UTC (a), 0222 UTC (b), 0223 UTC (c), and 0227 UTC (d).

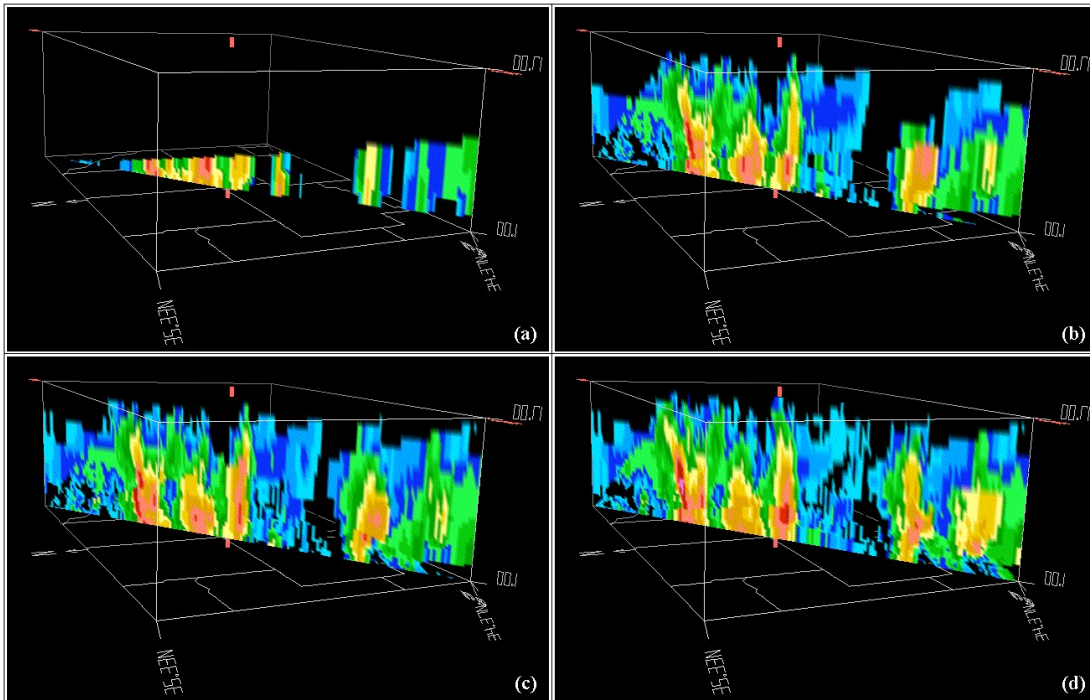


Fig. 6 4DDG output, with temporal weighting turned on, using KTLX and KFDR data on 14 August 2002. Shown is a vertical cross-section of 3-D reflectivity with endpoints at KTLX and KFDR at 0217 UTC (a), 0222 UTC (b), 0223 UTC (c), and 0227 UTC (d).

The 3D analysis aspects of the 4DDG are basically the same as those described in Zhang et al. (2004). Thus the new feature of 4DDG, the temporal weighting, is presented here. Illustrating this feature, Fig. 5 shows a four-panel of 4DDG output with its temporal weighting turned off. Meaning, the newest radar observations overwrite the old. Fig. 6 shows the same four-panel display with 4DDG's temporal weighting turned on. For both runs of 4DDG, the remap weighting scheme is 1-D vertical linear interpolation and the over-sampling weighting scheme is arithmetic mean.

Notice in Fig. 5 the discontinuities in the reflectivity field. This is most overt in Fig. 5b and Fig. 5d, where new reflectivity data from KTLX and KFDR overwrite older data. When compared to Fig. 6, the smoothing from 4DDG's temporal weighting is noticeable as tilts from KTLX and KFDR fill the 3-D grid. The storm structure at all four instances is better retained.

## 7. SUMMARY

The 4DDG algorithm and weighting schemes are presented in this paper. In addition, preliminary results are given. 4DDG ingests radar data as it becomes available on a tilt-by-tilt basis and uses spatial and temporal weighting schemes to continuously remap and mosaic radar data onto a 3-D grid.

Weighting schemes used by 4DDG are separated into three categories, remap, mosaic, and temporal. Both mosaic and temporal weights are based on an exponentially decaying weight function. The mosaic weighting scheme is dependent upon the distance of an observation from the radar. The temporal weighting scheme is based on the age of the observation.

Multiple remap weighting schemes are available and can be chosen via a user-defined option. Different remapping schemes are more appropriate for different applications. 4DDG's nearest neighbor scheme is good for research and development, but it leaves discontinuities and ring-shaped artifacts in the remapped field. The 1-D vertical linear interpolation is better for convective weather events. While this scheme reduces

the presence of ring-shaped artifacts some are still present for weather events involving stratiform precipitation. The 2-D horizontal linear interpolation scheme removes discontinuities in the remapped field, but can smear the vertical structure of convective storms. This scheme is best used for stratiform weather events.

4DDG has an additional set of weighting schemes to handle the over-sampling problem that occurs near a radar. Grid cells in close proximity to a radar are over-sampled because they are larger than their corresponding radar bins. A user-defined option determines if 4DDG uses an arithmetic mean or linear interpolation weighting method to smooth and include all observations in such instances. The over-sampled weights are incorporated into the remapping weights.

Preliminary results shown are from a severe storm case in Oklahoma on 14 August 2002. Data from WSR-88D radars, KTLX and KFDR, were used. 4DDG was run using 1-D vertical linear interpolation as the remap weight and arithmetic mean for the over-sampling weight. The temporal smoothing scheme is turned on and off to illustrate the effect of temporal smoothing on a 3-D mosaicked field.

## 8. ACKNOWLEDGMENTS

Major funding for this research was provided under the Aviation Weather Research Program NAPDT (NEXRAD Algorithms Product Development Team) MOU and partial funding was provided under NOAA-OU Cooperative Agreement #NA17RJ1227.

## 9. REFERENCE

- Doviak, R.J., and D.S. Zrnic, 1993: Doppler Radar and Weather Observations, 2<sup>nd</sup> Edition, Academic Press, 562 pp.
- Zhang, J., K. Howard, and J.J. Gourley, 2004: Constructing Three-dimensional Multiple Radar Reflectivity Mosaics: Examples of Convective Storms and Stratiform Rain Echoes, accepted for publication in *J. Atmos. Ocean. Tech*